

Ultra-wideband linear-to-circular polarizer realized by bi-layer metasurfaces: supplement

XI GAO,^{1,2}  KEXIN LI,¹ XIONGBIN WU,^{3,*} CHUNHUA XUE,¹  GUOFU WANG,¹ XIANMING XIE,¹ AND MIMI QIN¹

¹*School of Microelectronics and Materials Engineering, Guangxi University of Science and Technology, Liuzhou 545006, China*

²*Guangxi Key Laboratory of Precision Navigation Technology and Application, Guilin University of Electronic Technology, Guilin 541004, China*

³*Key Laboratory of Specialty Fiber Optics and Optical Access Networks, Shanghai University, Shanghai 200444, China*

*xb_wu2018@163.com

This supplement published with Optica Publishing Group on 11 May 2022 by The Authors under the terms of the [Creative Commons Attribution 4.0 License](https://creativecommons.org/licenses/by/4.0/) in the format provided by the authors and unedited. Further distribution of this work must maintain attribution to the author(s) and the published article's title, journal citation, and DOI.

Supplement DOI: <https://doi.org/10.6084/m9.figshare.19701550>

Parent Article DOI: <https://doi.org/10.1364/OE.460685>

Ultra-wideband Linear-to-Circular Polarizer Realized By Bi-layer Metasurfaces: supplemental document

To analyze the near-field coupling between two metasurfaces layers in detail, we decompose the proposed bi-layer metasurface [see Fig. 1(b)] to a four-layer system, as presented in Fig. 13(a). In the four-layer system, layer 1 and layer 2 (layer 3 and layer 4) are respectively spaced by an air gap with thickness of t_0 ($t_0=0$). When this four-layer system is normally illuminated by a x-polarized plane wave, each metasurface layer will generate induced currents, as presented in Fig. S1(b). According to ref. [1], the induced current density vector ($\vec{J}_p(\rho, \omega)$) of layer p ($p=1,2,3,4$) is denoted as

$$\begin{cases} \vec{J}_1(\rho, \omega) = c_1(\omega) \vec{J}_1(\rho) \\ \vec{J}_2(\rho, \omega) = c_2(\omega) \sum_l \vec{J}_2(\rho - \rho_l) \\ \vec{J}_3(\rho, \omega) = c_2(\omega) \sum_l \vec{J}_2(\rho - \rho_l) \\ \vec{J}_4(\rho, \omega) = c_1(\omega) \vec{J}_1(\rho) \end{cases} \quad (S1)$$

where $\vec{J}_1(\rho)$ is the induced current density vector on the metal strip along the x-direction, and $\sum_l \vec{J}_2(\rho - \rho_l)$ ($l = 1, 2, 3, 4$) is the induced current density vector on Jerusalem-cross-like resonator [see layer 2 in Fig. S1(b)]. It is noted that $c_{s(s=1,2)}(\omega)$ is frequency-dependent complex amplitude coefficient, $\vec{J}_{s(s=1,2)}(\rho)$ is the spatial profile of current, and $\rho_{l(l=1,2,3,4)}$ is the position of the l th scatterer. The currents $\vec{J}_1(\rho)$ and $\vec{J}_2(\rho - \rho_l)$ are independent of ω and they can be solved by using the eigenmode solver in commercial software CST Microwave Studio.

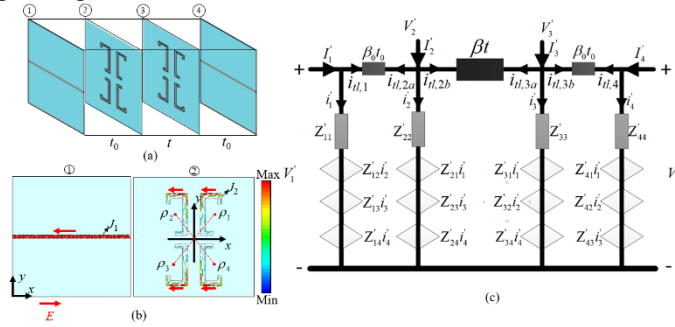


Fig. S1. (a) The decomposed four-layer metasurface. (b) Surface current distributions of layer 1 and layer 2. (c) The equivalent circuit model of the four-layer system.

The self-impedance in Fig. S1(c) can be written as

$$\begin{aligned} Z'_{ii(i=1,2)} &= \sum_{qmn(m,n) \neq (0,0)} \frac{M_{i,q}^2 \left[(Y_q^1 + Y_q^2) - (Y_q^1 - Y_q^2) e^{-2j\beta_{mt}t} \right]}{(Y_q^1 + Y_q^2)^2 - (Y_q^1 - Y_q^2)^2 e^{-2j\beta_{mt}t}}, \\ Z'_{11} &= Z'_{44}, Z'_{22} = Z'_{33} \end{aligned} \quad (S2)$$

and the mutual impedance can be written as

$$\left. \begin{aligned}
Z'_{12} &= Z'_{21} = Z'_{34} = Z'_{43} \\
Z'_{12} &= \sum_{qmn(m,n) \neq (0,0)} \frac{M_{1,q} M_{2,q}^* 2Y_q^2}{(Y_q^1 + Y_q^2)^2} \\
Z'_{14} &= Z'_{41}, \quad Z'_{23} = Z'_{32} \\
Z'_{14} &= \sum_{qmn(m,n) \neq (0,0)} \frac{M_{1,q} M_{1,q}^* (2Y_q^2 e^{-j\beta_{mn}t})}{(Y_q^1 + Y_q^2)^2 - (Y_q^1 - Y_q^2)^2 e^{-2j\beta_{mn}t}} \\
Z'_{23} &= \sum_{qmn(m,n) \neq (0,0)} \frac{M_{2,q} M_{2,q}^* (2Y_q^2 e^{-j\beta_{mn}t})}{(Y_q^1 + Y_q^2)^2 - (Y_q^1 - Y_q^2)^2 e^{-2j\beta_{mn}t}} \\
M_{1,q} &= \left(\tilde{J}_1(\mathbf{k}_{t,q}) \cdot \vec{e}_q \right) / \left(\tilde{J}_1(\mathbf{k}_0) \cdot \vec{e}_q \right), \quad M_{2,q} = \left(\tilde{J}_2(\mathbf{k}_{t,q}) \cdot \vec{e}_q \right) / \left(\tilde{J}_2(\mathbf{k}_0) \cdot \vec{e}_q \right)
\end{aligned} \right\}, \quad (S3)$$

where β_{mn} is the propagation constants of nm th harmonics ($m, n=0$), Y_q^1 and Y_q^2 is the admittance of the Floquet harmonic in free space and in dielectric layer, respectively. For TM harmonics, $\vec{e}_q = \left(k_{xn} \vec{e}_x + k_{ym} \vec{e}_y \right) / \sqrt{k_{xn}^2 + k_{ym}^2}$, and for TE harmonics, $\vec{e}_q = \left(k_{ym} \vec{e}_x - k_{xn} \vec{e}_y \right) / \sqrt{k_{xn}^2 + k_{ym}^2}$. \tilde{J}_1 (\tilde{J}_2) is the Fourier transform of the current on layer 1 (layer 2),

$$\tilde{J}_i(k_{t,q}) = \int_{u,c} \vec{J}_i(\rho) e^{jk_{t,q}\rho} d\rho \quad (S4)$$

Similar to Eq. (2) in Main Text, equivalent voltages V'_n and i'_n ($n = 1, 2, 3, 4$) are also denoted by the near-field impedance matrix $[Z']$,

$$\begin{bmatrix} i'_1 \\ i'_2 \\ i'_3 \\ i'_4 \end{bmatrix} = \begin{bmatrix} Z'_{11} & Z'_{12} & Z'_{13} & Z'_{14} \\ Z'_{21} & Z'_{22} & Z'_{23} & Z'_{24} \\ Z'_{31} & Z'_{32} & Z'_{33} & Z'_{34} \\ Z'_{41} & Z'_{42} & Z'_{43} & Z'_{44} \end{bmatrix}^{-1} \begin{bmatrix} V'_1 \\ V'_2 \\ V'_3 \\ V'_4 \end{bmatrix} = \begin{bmatrix} Y'_{11} & Y'_{12} & Y'_{13} & Y'_{14} \\ Y'_{21} & Y'_{22} & Y'_{23} & Y'_{24} \\ Y'_{31} & Y'_{32} & Y'_{33} & Y'_{34} \\ Y'_{41} & Y'_{42} & Y'_{43} & Y'_{44} \end{bmatrix} \begin{bmatrix} V'_1 \\ V'_2 \\ V'_3 \\ V'_4 \end{bmatrix}. \quad (S5)$$

Owing to $t_0=0$, layer 1 and layer 2 are overlapped. Hence the voltage V'_1 is approximately equal to V'_2 . Similarly, $V'_3 = V'_4$. In this case (S5) can be written as

$$\begin{bmatrix} i'_1 \\ i'_2 \\ i'_3 \\ i'_4 \end{bmatrix} = \begin{bmatrix} Y'_{11} & Y'_{12} & Y'_{13} & Y'_{14} \\ Y'_{21} & Y'_{22} & Y'_{23} & Y'_{24} \\ Y'_{31} & Y'_{32} & Y'_{33} & Y'_{34} \\ Y'_{41} & Y'_{42} & Y'_{43} & Y'_{44} \end{bmatrix} \begin{bmatrix} V'_1 \\ V'_1 \\ V'_4 \\ V'_4 \end{bmatrix}, \quad (S6)$$

Through a simple calculation process, Eq. (S6) can be reduced into a 2×2 matrix.

$$\begin{bmatrix} i_a \\ i_b \end{bmatrix} = \begin{bmatrix} i'_1 + i'_2 \\ i'_3 + i'_4 \end{bmatrix} = \begin{bmatrix} Y_{11}^{eq} & Y_{12}^{eq} \\ Y_{21}^{eq} & Y_{22}^{eq} \end{bmatrix} \begin{bmatrix} V'_1 \\ V'_4 \end{bmatrix} = \begin{bmatrix} Z_{11}^{eq} & Z_{12}^{eq} \\ Z_{21}^{eq} & Z_{22}^{eq} \end{bmatrix}^{-1} \begin{bmatrix} V'_1 \\ V'_4 \end{bmatrix}, \quad (S7)$$

where $Y_{11}^{eq} = Y'_{11} + Y'_{12} + Y'_{21} + Y'_{22}$, $Y_{12}^{eq} = Y'_{13} + Y'_{14} + Y'_{23} + Y'_{24}$, $Y_{21}^{eq} = Y'_{31} + Y'_{32} + Y'_{41} + Y'_{42}$, and $Y_{22}^{eq} = Y'_{33} + Y'_{34} + Y'_{43} + Y'_{44}$. Actually, Eq. (S6) is identical with Eq. (2). The currents i_a and i_b are respectively equal to i_1 and i_2 in Eq. (2). Correspondingly, the voltages V'_1 and V'_4 are respectively equal to V_1 and V_2 , and $\begin{bmatrix} Y_{11}^{eq} & Y_{12}^{eq} \\ Y_{21}^{eq} & Y_{22}^{eq} \end{bmatrix}$ is equal to $\begin{bmatrix} Y_{11} & Y_{12} \\ Y_{21} & Y_{22} \end{bmatrix}$ in Eq. (2). Up to now the $[Z]$ matrix presented in Eq. (2) can be obtained from the $[Y']$ matrix shown in Eq. (S5). Unlike those reported methods, we can obtain the S parameters of multilayer metasurfaces only by

calculating the current distributions of each single-layer metasurface, thereby effectively decreasing the requirement of computer.

References

1. Gao X, Wu X, Li K, et al, "Accurate semi-numerical approach for multilayer metasurfaces with near-field coupling," Opt. Express 29(25), 42225-42237 (2021).